VNU Journal of Science: Mathematics – Physics, Vol. 36, No. 4 (2020) 1-9

VNU Journal of Science: Mathematics - Physics

Journal homepage: https://js.vnu.edu.vn/MaP

Original Article

Fabrication of Ba Doped $LaMnO_3$ Nanomaterials by Microwave Combustion Method

Tran Thi Ha[1], Pham Nguyen Hai[2], Tran Thi Uyen[2], Nguyen Ngoc Dinh[2], Nguyen Thi Ha Thu[3], Ho Khac Hieu[4,5], Nguyen Viet Tuyen[2,*]

[1]*Faculty of Basic Sciences, Hanoi University of Mining and Geology, 18 Vien, Duc Thang, Hanoi, Vietnam*

[2]*Faculty of Physics, VNU University of Science, 334 Nguyen Trai, Thanh Xuan, Hanoi, Vietnam*

[3]*Air Defence -Air Force Academy, Kim Son, Son Tay, Hanoi, Vietnam*

[4]*Institute of Research and Development, Duy Tan University, 03 Quang Trung, Da Nang, Vietnam*

[5]*Faculty of Natural Sciences, Duy Tan University, 03 Quang Trung, Hai Chau, Da Nang, Vietnam*

Received 29 February 2020
Revised 27 April 2020; Accepted 30 June 2020

Abstract: The major energy sources that human are relying on are fossil fuel and it is exhausted day by day. Furthermore, exploition and usage of fossil fuel also bring in many negative impacts on environmental polution. Solid oxide fuel cell (SOFC) has been considerred as a potential solution for such environmental and energy problems. Seeking a facile, cost and time saving process to synthesize Ba doped $LaMnO_3$ is very important for development of SOFC applications because it helps to reduce the cost of comercial SOFC. $LaMnO_3$ doped with Ba is more cost effective than Sr doped $LaMnO_3$ because less rare earth elements are used. At the same time, its conductivity is still good enough with an appropriate thermal expansion matched with those of other parts of SOFC based on ytrium stabilized zirconia (YSZ).

In this paper, Ba doped $LaMnO_3$ nanoparticles (LBMO), a promissing material for making cathode of SOFC, were prepared by microwave combustion method. This material has many advantages. Effect of the amount fuel in the combustion reaction on the products was studied by various methods such as: X-ray diffraction measurement, scanning electron microscopy, energy dispersive X-ray spectroscopy. The results showed that each doping rate requires an appropriate amount of fuel to obtain pure and crystalline product. The obtained LBMO nanoparticles are crystallined in hexagonal phase at doping ratio of 0.2 and orthohombic phase at doping ratio of equal or larger than 0.3.

Keywords: Perovskite, microwave combustion, Ba doped $LaMnO_3$ nano particle.

*Corresponding author.
Email address: nguyenviettuyen@hus.edu.vn

https//doi.org/ 10.25073/2588-1124/vnumap.4471

1. Introduction

In the next several decades, minimizing emission gases due to burning fossil fuels is extremely important to reduce the impact on environment polution. A promising solution is SOFC because it can transform energy from chemical bonding of fuel (bio-gas, natural gas, hydrogen, etc. directly into electricity via electrochemical reactions at high yield while reduce much toxic emission gases [1–4]. The most commonly used materials in cathode of SOFC are ABO_3 perovskites, where A is a rare earth metal (La, Sr, etc.) and B is a transition metals such as: Mn, Fe, Co, Ni or the combination of these metals [2, 5–7]. The catalytic ability of oxidation reduction process is provided by cation B. With an appropriate selection of A and B, a number of oxygen vacancies are generated during working process and thus support for the transport of a large amount of oxygen to the electrolyte layer [8–12]. Lanthanum manganite is a perovskite with p type conduction, fulfills the requirements for cathodes of SOFC, which are high conductivity, suitable thermal expansion, stability in both oxidized and reduced ambient at high temperature [8, 9]. Recently, Ba was reported as a promissing dopant, which can help to increase the conductivity and magnetic property of $LaMnO_3$ [15–18].

In this research, Ba which is an earth alkali metal of abundant amount and low cost, was a doped into $LaMnO_3$ with the hope that partial replacement of rare earth elements with low cost one can help to gain better price and electrical properties of cathode of SOFC .

2. Experiment

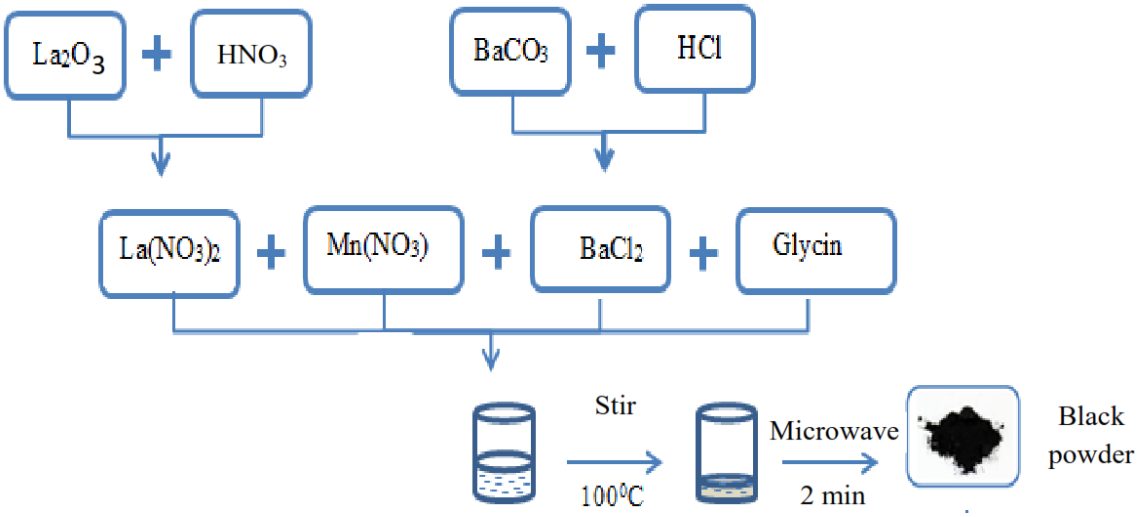

Figure 1. Diagram of synthetic process of LBMO by microwave combustion method.

The synthetic process is summarized in the diagram shown in Figure 1. Precursor materials are La_2O_3 (99.99%), $Mn(NO_3)_2.4H_2O$ (99%) and glycine NH_2CH_2COOH (99%). La_2O_3 was dissolved in HNO_3 acid (65%) to obtain $La(NO_3)_3$ solution. Then, $La(NO_3)_3$, $Ba(NO_3)_2.4H_2O$ and $Mn(NO_3)_2.4H_2O$ were mixed together to form a solution with La : Ba : Mn molar ratio of (1-x) : x : 1 where x = 0.2; 0.3; 0.5; 0.6; 0.7 is the doping rate. In the next step, glycine of appropriate amount was added to the solution. A set of $La_{1-x}Ba_xMnO_3$ samples was prepared and denoted as BxGy where, x is the doping

rate and y is defined as molar ratio between glycine and Mn. The obtained solution would be heated by a magnetic stirrer at 100 ºC. After 40 min the color of solution would turn into milky gel. The gel was transferred into a microwave oven and heated in 2 min at power of 800 W. The microwave supported for the combustion reaction and produced black powder.

3. Results and Discussion

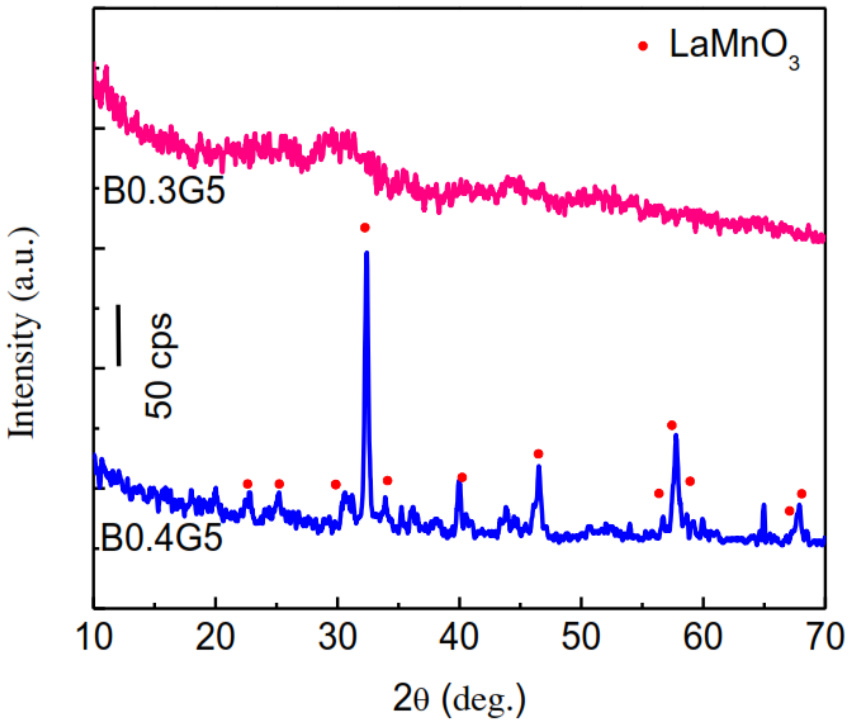

Figure 2. XRD patterns of LBMO power samples with doping rate x = 0.3 and 0.4.

Glycine plays an important role in the formation of metal complexes, which guarantees a homogenous reaction at atomic level. Moreover, glycine supports for the reduction of nitrate group in combustion process and liberates a huge amount of heat for the formation of pervoskite crystal. Hence, investigating the effect of fuel amount on structure and morphology of nanoproduct prepared by microwave combustion is very important. A small amount of fuel which is below threshold will not provide enough energy for the reaction to occur. On the other hand, excess amount of fuel will also degrade the quality of the product because generated gas in the reaction will dissipate the useful heat for the reaction. Simultaneously, doping concentration also changes kinetics of reaction. The XRD results (Figure 2) show that when same amount fuel is utilized (y=5), the quality of the product changes a lot depending on the doping rate (x = 0.3 or 0.4). XRD diffraction patterns show that $La_{0.6}Ba_{0.4}MnO_3$ sample was in crystalline form, implied by characteristic peaks of $LaMnO_3$, without dopant or impurity. Meanwhile, sample $La_{0.7}Ba_{0.3}MnO_3$ was amorphous even though the same ratio of fuel to precursors was applied. Thus, $La_{0.7}Ba_{0.3}MnO_3$ nanomaterial was prepared with three different y values: 4.5; 4.75 and 5. It should be noted that y of less than 4.5 resulted in non crystalline product as demonstrated by XRD patterns in Figure 3.

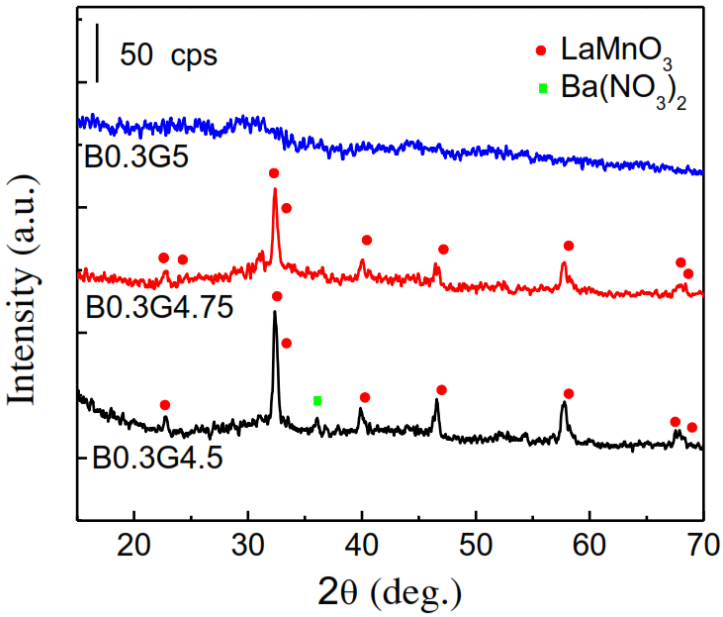

Figure 3. XRD patterns of $La_{0.7}Ba_{0.3}MnO_3$ powder prepared with different value of y: 4.5; 4.75 and 5.

The above results suggest that each doping rate x will require a corresponding appropriate fuel to precursors ratio.

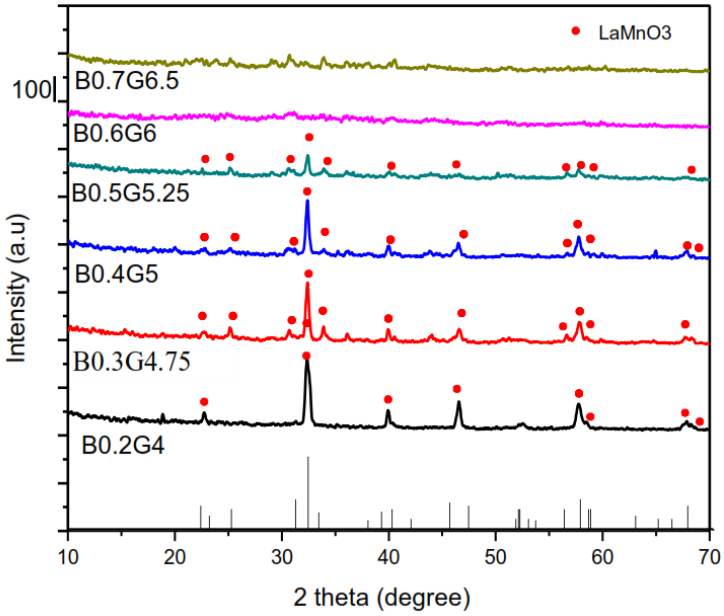

Figure 4. XRD patterns of LBMO samples of different doping rate x= 0.2; 0.3; 0.4; 0.5; 0.6; 0.7.

The detailed investigation showed that fuel ratio of y = 4 offers $La_{0.8}Ba_{0.2}MnO_3$ of hexagonal phase. For samples with doping rate x = 0.3; 0.4; 0.5, the fuel to precursor ratio y equals 4.75; 5; 5.25

respectively will produce single phase nanopowder of orthorhombic structure. Samples with doping rate x greater than 0.6 can not be obtained in crystalline form at any value of fuel ratio y. These results are in agreement with theoretical calculation by Ahmed [19], where the authors showed that the greater the doping concentration is the harder for the product can be formed due to the difference in ion radius of Ba and La. Ahmed et al. calculated the dependence of formation energy of LBMO materials on doping rate. The results are summarized in Table 1.

Table 1. Forming energy of LBMO product of different doping rate [19].

X	0.125	0.25	0.375	0.5	0.625	0.75	0.875
E_{form} (meV/atom)	438.2	518.6	588.0	676.1	773.5	883.9	984.6

A high formation energy implies difficulties of doping process. As doping rate increases, the formation energy grows correspondingly. Thus, a high doping rate will require more heat provided by fuel. However, the gas product dissipates some portion of heat to environment, which is not useful for the combustion reaction. This explains for the optimum value of fuel ratio for each doping concentration as investigated above.

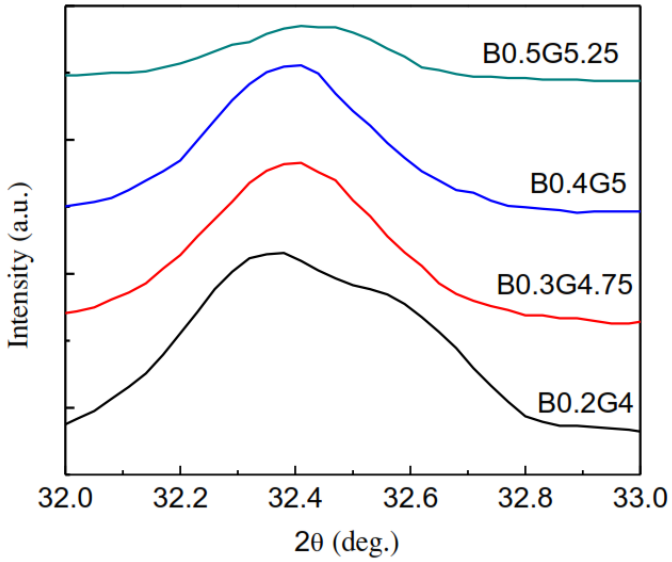

Figure 5. XRD patterns of LBMO samples with doing rate x = 0.2; 0.3; 0.4; 0.5 in a 2theta range of 32 and 33°.

As can be seen from Figure 5, the strongest peak of LBMO shows a clear shift toward higher angle as the doping concentration increases. This peak shift is an indication of replacement of La in the lattice by Ba ion. The decreasement of distance between two neighbor planes with increasing of doping concentration can be explained by the smaller radius of Ba^{2+} ion compared with that of La. The lattice parameters of LBMO samples were estimated by using the following formula for distances between neighbor planes of orthorhombic and hexagonal structures, while the crystal size was

estimated by Sherrer formula. The estimated data (shown in Table 2) are in consistent with the values reported in literature for $LaMnO_3$ materials [3, 11].

Table 2. Lattice parameters and crystal size of LBMO samples of different doping concentration x = 0.2; 0.3; 0.4; 0.5.

Sample	a	b	c	D	Phase
$La_{0.8}Ba_{0.2}MnO_3$	4.147Å	4.147 Å	13.463 Å	19.60nm	Hexagonal
$La_{0.7}Ba_{0.3}MnO_3$	5.523 Å	5.698 Å	7.803 Å	21.61nm	Orthorhombic
$La_{0.6}Ba_{0.4}MnO_3$	5.523 Å	5.680 Å	7.790 Å	24.43nm	Orthorhombic
$La_{0.5}Ba_{0.5}MnO_3$	5.482 Å	5.678 Å	7.736Å	26.44nm	Orthorhombic

Elemental percentage of the nanoproducts determined by EDS spectra agrees well with the nominal content of the starting materials. For example, in the obtained $La_{0.8}Ba_{0.2}MnO_3$ sample (Figure 6), the atomic element ratio of La, Ba and Mn is 8 : 2 : 9.3. This is close to the stoichiometric ratio 8 : 2 : 10.

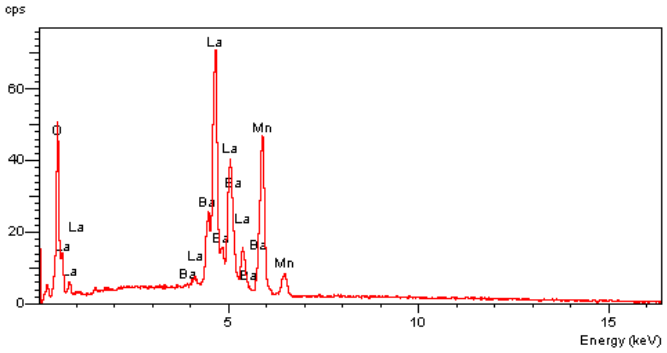

Figure 6. EDS spectrum of LBMO sample with x=0.2.

When doping Ba into $LaMnO_3$ lattice, Ba can either replace for La or go into interstition position, stay at the grain boundary, or dissociate to form another phase of Ba for instance $BaCO_3$. However, the combination of XRD and EDS data suggest that the second case can be neglected because the amount of Ba in the product consists with the nominal doping concentration while the product are single phase even at high doping concentration.

Microstructure of the product can affect greatly to the catalyst yield of ceramic materials, thus, the micromorphology of the samples was investigated by scanning electron microscope. The SEM images in Figure 7 show that the obtained products are nanoparticles in range of 100–300 nm. The uniform particle size demonstrates the potential of using the nanoproduct as a precursor materials for fabrication of thin films of perovskite for cathode of SOFC.

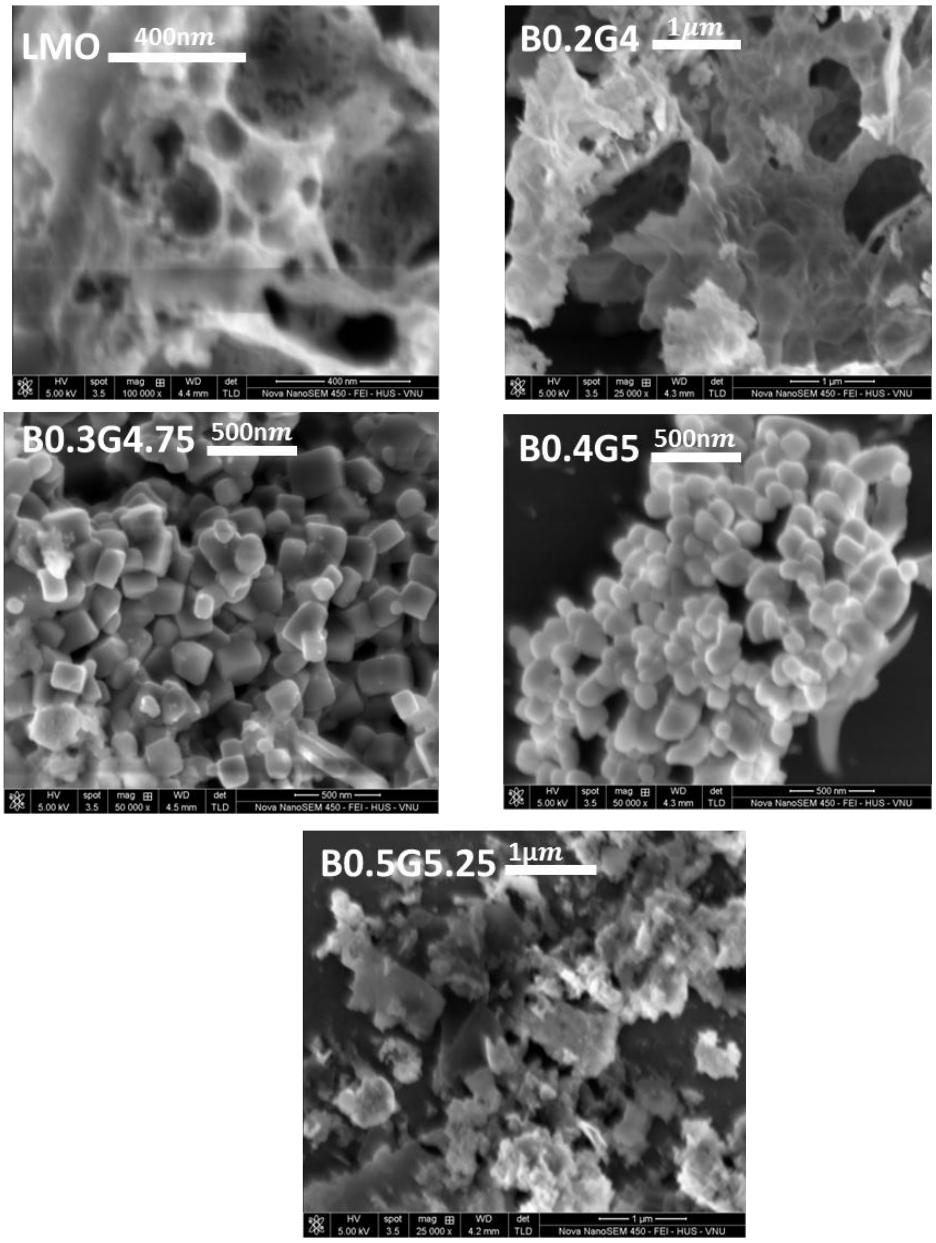

Figure 7. SEM images of LBMO samples with x= 0.2; 0.3; 0.4; 0.5.

4. Conclusion

Ba doped $LaMnO_3$ nanopowder was prepared by microwave combustion method with many advantages such as: simple setup, low cost, time saving. The study showed that glycine as the fuel of the combustion reaction plays a critical role on the formation of perovskite nanomaterials. A fine control of fuel amout is necessary for the production of single phase product. The preparation of Ba

doped $LaMnO_3$ nanoparticles of single phase, high quality opens the possiblilty to fabricate nanocrystalline thin films of this material by electrophoresis for SOFC applications.

Acknowledgments

This research is funded by the Vietnam National Foundation for Science and Technology Development (NAFOSTED) under grant number 103.01-2017.343. One of the authors, PhD student Thi Ha Tran, would like to thank the Domestic Master/ PhD Scholarship Programme of Vingroup Innovation Foundation for supporting tuition fee.

References

[1] A. Tarancón, Strategies for lowering solid oxide fuel cells operating temperature, Energies. 2 (2009) 1130–1150. https://doi.org/10.3390/en20401130.

[2] A.M. Abdalla, S. Hossain, A.T. Azad, P.M.I. Petra, F. Begum, S.G. Eriksson, A.K. Azad, Nanomaterials for solid oxide fuel cells: A review, Renew. Sustain. Energy Rev. 82 (2018) 353–368. https://doi.org/10.1016/j.rser.2017.09.046.

[3] T.H. Tran, T.C. Bach, N.H. Pham, Q.H. Nguyen, C.D. Sai, H.N. Nguyen, V.T. Nguyen, T.T. Nguyen, K.H. Ho, Q.K. Doan, Phase transition of $LaMnO_3$ nanoparticles prepared by microwave assisted combustion method, Mater. Sci. Semicond. Process. 89 (2019) 121–125. https://doi.org/10.1016/j.mssp.2018.09.002.

[4] T.H. Tran, T.T.A. Tang, N.H. Pham, T.C. Bach, C.D. Sai, Q.H. Nguyen, V.V. Le, H.N. Nguyen, Q.K. Doan, T.T. Nguyen, V.B. Le, K.H. Ho, V.T. Nguyen, A novel approach for fabricating $LaMnO_3$ thin films using combined microwave combustion and pulsed electron deposition techniques, J. Chem. 2019 (2019) 1–8. https://doi.org/10.1155/2019/3568185.

[5] H. Xu, B. Chen, P. Tan, W. Cai, W. He, D. Farrusseng, M. Ni, Modeling of all porous solid oxide fuel cells, Appl. Energy. 219 (2018) 105–113. https://doi.org/10.1016/j.apenergy.2018.03.037.

[6] M. Riazat, M. Baniassadi, M. Mazrouie, M. Tafazoli, M. Moghimi Zand, The Effect of cathode Porosity on Solid Oxide Fuel Cell Performance, Energy Equip. Syst. 3 (2015) 25–32. https://doi.org/10.22059/ees.2015.13908.

[7] B. Zhu, B. Wang, Y. Wang, R. Raza, W. Tan, J.S. Kim, P.A. van Aken, P. Lund, Charge separation and transport in $La_{0.6}Sr_{0.4}Co_{0.2}Fe_{0.8}O_{3-\delta}$ and ion-doping ceria heterostructure material for new generation fuel cell, Nano Energy. 37 (2017) 195–202. https://doi.org/10.1016/j.nanoen.2017.05.003.

[8] S. Daengsakul, C. Thomas, I. Thomas, C. Mongkolkachit, S. Siri, V. Amornkitbamrung, S. Maensiri, Magnetic and cytotoxicity properties of $La_{1-x}Sr_xMnO_3 (0 \leq x \leq 0.5)$ nanoparticles prepared by a simple thermal hydro-decomposition, Nanoscale Res. Lett. 4 (2009) 839–845. https://doi.org/10.1007/s11671-009-9322-x.

[9] J. Rodríguez-Carvajal, M. Hennion, F. Moussa, L. Pinsard, A. Revcolevschi, The Jahn-Teller structural transition in stoichiometric $LaMnO_3$, Phys. B Condens. Matter. 234–236 (1997) 848–850. https://doi.org/10.1016/S0921-4526(96)01122-2.

[10] N.H. Nam, D.T.M. Huong, N.H. Luong, Synthesis and Magnetic Properties of Perovskite $La_{1-x}Sr_xMnO_3$ Nanoparticles, Ieee Trans. Magn. 50 (2014) 3–6. https://doi.org/Artn 2503104 10.1109/Tmag.2014.2307834.

[11] J. He, J. Sunarso, Y. Zhu, Y. Zhong, J. Miao, W. Zhou, Z. Shao, High-performance non-enzymatic perovskite sensor for hydrogen peroxide and glucose electrochemical detection, Sensors Actuators, B Chem. 244 (2017) 482–491. https://doi.org/10.1016/j.snb.2017.01.012.

[12] T.M.K. Thandavan, S.M.A. Gani, C.S. Wong, R.M. Nor, Enhanced photoluminescence and Raman properties of Al-doped ZnO nanostructures prepared using thermal chemical vapor deposition of methanol assisted with heated brass, PLoS One. 10 (2015) 1–18. https://doi.org/10.1371/journal.pone.0121756.

[13] T.T. Ha, T. Thi, T. Anh, P.T. Linh, P.T. Huong, P.N. Hai, N.H. Nam, B.T. Cong, S.C. Doanh, N.Q. Hoa, D. Van, L.V. Bau, H.K. Hieu, D.Q. Khoa, N.V. Tuyen, Pulsed electron deposition of $LaMnO_3$ thin films with target made of $LaMnO_3$ nano-powder synthesized by self combustion method, in: Proc. IWNA 2017, 08-11 Novemb. 2017, Phan Thiet, Vietnam, Phan Thiet, 2017: pp. 203–206.

[14] N.V.T. Phi Thi Huong, Pham Thuy Linh, Tran Thi Uyen, Nguyen Hoang Nam, Tran Thi Ha, Ho Khac Hieu, Preparation of Sr doped $LaMnO_3$ nanoparticles by microwave combustion method, DTU J. Sci. Technol. 5 (2018) 74–79.

[15] S.I. Patil, M.S. Sahasrabudhe, S.N. Sadakale, P.R. Sagdeo, R.N. Bathe, K.P. Adhi, S.K. Date, S.M. Bhagat, Phase separation scenario in Ba doped $LaMnO_3$, Phys. Status Solidi C Conf. 1 (2004) 3623–3627. https://doi.org/10.1002/pssc.200405518.

[16] A.L. Gavin, G.W. Watson, Defects in orthorhombic $LaMnO_3$-ionic: Versus electronic compensation, Phys. Chem. Chem. Phys. 20 (2018) 19257–19267. https://doi.org/10.1039/c8cp02763c.

[17] S.M. Ramay, A. Mahmood, S. Atiq, A.N. Alhazaa, Study of divalent elements (Mg, Sr and Ba)-doped $LaMnO_3$ nano-manganites, Int. J. Mod. Phys. B. 30 (2016) 1–9. https://doi.org/10.1142/S021797921650020X.

[18] R. Dhama, C. Nayek, C. Thirmal, P. Murugavel, Enhanced magnetic properties in low doped $La_{1-x}Ba_xMnO_{3+\delta}$ (x=0, 0.1 and 0.2) nanoparticles, J. Magn. Magn. Mater. 364 (2014) 125–128. https://doi.org/10.1016/j.jmmm.2014.04.010.

[19] N. Ahmed, S. Khan, A.A. Khan, A.G. Nabi, H. Ahmed, Z. ur Rehman, M.H. Nasim, Synthesis, structural, electronic, and magnetic properties of cubic perovskite $La_{1-x}Ba_xMnO_3$ ($0.125 \leq x \leq 0.875$) for spintronic devices, J. Supercond. Nov. Magn. 31 (2018) 4079–4089. https://doi.org/10.1007/s10948-018-4691-y.

[20] M.S.-N. Maryam Shaterian, Morteza Enhessari, Davarkhah Rabbani, Morteza Asghari, Synthesis, characterization and photocatalytic activity of $LaMnO_3$ nanoparticles, Appl. Surf. Sci. 318 (2014) 213–217. https://doi.org/10.1080/10934529.2013.824789.